Materials Research. 2016; 19(6): 1381-1387
DOI: http://dx.doi.org/10.1590/1980-5373-MR-2015-0733

Synthesis and Structural Properties of Niobium Pentoxide Powders: A Comparative Study of the Growth Process

***Angela M. Raba*[a], *Jorge Bautista-Ruíz*[a], *Miryam R. Joya*[b,*]**

[a] *Departamento de Física, Universidad Francisco de Paula Santander, Cucuta, North Santander, Colômbia*
[b] *Departamento de Física, Facultad de Ciencias, Universidad Nacional de Colombia, Cra 45, Bogotá, Colômbia*

Received: December 02, 2015; Revised: August 23, 2016; Accepted: September 10, 2016

Powders Nb_2O_5 were prepared by two different synthesis method, Sol-Gel and polymeric precursors (Pechini). In the Pechini method before adding the citric acid in the process, four different solutions were used to get the samples. For Sol-gel method, two different processes were also used in obtaining powders. The precursor was completely solubilized in ethanol and then hydrolyzed with ammonia and water. The calcination of the samples was between 500 and 750°C. The resulting powders were characterized by Scanning Electron Microscopy (SEM), Brunauer, Emmett and Teller (BET) surface area measurements, UV-visible and Raman spectroscopy. The formation of T−Nb_2O_5 orthorhombic took place upon calcination at 750ºC. Crystallite sizes were determined using the Scherrer method which resulted in an uniformed size of about 25 − 65nm. Ultraviolet-Visible diffuse reflectance spectroscopy indicated a variation in the optical band gap values (3.32-3.40 eV) in crystal growth process. The Raman vibrational modes indicate the presence of the orthorhombic phase of the material.

Keywords: *comparative study, sol-gel, Uv-Vis, Inelastic light scattering and* Nb_2O_5

1. Introduction

Niobium Pentoxide (Nb_2O_5) is an *n*-type semiconductor with a band gap of about 3.4 *eV*, low in comparison to other oxides. The interest in studying the Nb_2O_5 is due to its remarkable physicochemical properties and structural isotropy suitable for a wide range of applications in the construction of gas sensing, electrochromics display and photoelectrodes, as well as in field-emission displays and microelectronics[1-6]. Studies were conducted in the past on the use of Nb_2O_5 nanoparticles for environmental remediation in water through of photocatalytic processes. In these technologies Nb_2O_5 shows great potential because of its stability in an aqueous medium, its surface acidity, redox and photocatalytic properties, which are instrinsically linked to its structure[7-9].

The main phases reported in literature for Nb_2O_5 are TT-Nb_2O_5 (pseudohexagonal) at low temperatures, T-Nb_2O_5 (orthorhombic structure) heating the amorphous oxide to 600 and 800°C, and H-Nb_2O_5 (monoclinic structure) heating to about 1100°C [10]. In general the crystallization conditions of each Nb_2O_5 structure depends on the starting materials, synthesis methods and heat treatment conditions. In particular the T-Nb_2O_5 net parameters are: $a = 6.17$Å; $b = 29.32$Å; $c = 3.94$Å, and its crystalline structures consist of 4 × 4 blocks of corner-shared NbO_6 octahedra, with connected blocks sharing the edges of the octahedron[11].

In order to get thin films of Nb_2O_5 there are two phase deposition methods. Liquid phase deposition and vapour phase deposition. For the liquid phase methods such as hydrothermal, solvothermal, anodization, sol-gel and electrodeposition exist and the physical and chemical methods for the vapour phase[12]. Additionally, nanostructures of Nb_2O_5 are obtained through sol-gel and precipitation methods. Besides, the preparation of niobium base materials also the Pechini route is used.

Soares et al.[11] reported the synthesis of Nb_2O_5 samples by means of the Laser Floating Zone (LFZ) technique and the solid-state reaction in order to study some of their physical properties as a function of synthesis conditions. The authors found a structural orthorhombic to monoclinic phase transition observed in samples sintered at temperatures higher than 800°C. Rosario et al.[13] prepared Nb_2O_5 powders and films using the niobium salt $NH_4H_2[NbO(C_2O_4)_3].3H_2O$ as starting material. Nb_2O_5 nanoparticles obtained by the oxidant-peroxo method[14] were synthesized employing ammonium niobium oxalate ($NH_4[NbO(C_2O_4)_2(H_2O)_2].nH_2O$ as a starting precursor. These nanoparticles presented mixed phases of Nb_2O_5 orthorhombic and $Nb_2O_5\,nH_2O$. Sol- gel methods have been widely reported in the production of porous and high surface area niobium oxides. Molecular precursors, mainly metal alkoxides, are generally used as starting materials. In the work[15] Nb_2O5 amorphous powders prepared by the Sol-gel technique and their crystalline structures were analyzed through a controlled heat-treatment process. Ristic et al.[16] reported that the $Nb(OC_2H_5)_5$ was used as a starting precursor in the preparation of the Nb_2O_5 powders using the Sol-gel procedure. The initial Nb_2O_5

* e-mail: mrinconj@unal.edu.co

powders were amorphous and by heating them at 500° C contained Nb_2O_5 (TT-phase), whereas at 650°C the Nb_2O_5 (T-phase) was obtained. Uekawa et al.[17] reported that the synthesis of highly crystallized Nb_2O_5 nanoparticles with a diameter of 4.5*nm* was based also on a Sol-gel route.

In this research, Nb_2O_5 nanosize powders were prepared by two different routes: a) the Sol-gel technique, for its similarities with the Pechini route (in other research also known as the citrate gel route[15]) and b) the Pechini method, using different sintering temperatures (500-750°C). The powders obtained were characterized by X-ray diffraction (*XRD*) to evaluate the influence of heat treatment on the formation of the TT- Nb_2O_5 and T-Nb_2O_5 phases. Also by the *BET* method in order to obtain measurements of surface area, the UV-vis diffuse reflectance spectroscopy (*DRS*) to identify the band gap energy and the Raman spectroscopy to perform a vibrational characterization.

2. Experimental details

2.1. Preparation of the nanosize powders

Tables of the synthesis procedure are shown in (1) and (2). The samples 1−Nb_2O_5 and 2−Nb_2O_5 were synthesized by the Sol-gel method according to literature procedures[16]. Niobium (V) ethoxide, ($Nb(OC_2H_5)_5$ 99.999% Alfa Aesar) was employed as the starting precursor and absolute ethanol for analysis (Merck) and Ammonia hidroxide 30% (Panreac) were also used. The samples 1−Nb_2O_5 were prepared by adding 5*g* of $Nb(OC_2H_5)_5$ to 90*ml* of absolute ethanol which was stirred vigorously, then 5*ml* of Ammonia hydroxide was added to the precipitation system. The samples 2−Nb_2O_5 were prepared by adding 5*g* of $Nb(OC_2H_5)_5$ to 94*ml* of absolute ethanol under vigorous stirring, then 1*ml* of distilled water was added to the precipitation system. After firmly shaking, the precipitation systems were transferred to petri dishes and left to evaporate at 60°C on a stove; the solid residue was subsequently dried at 160°C for 4h in an oven. The powders obtained were calcined at 500, 650 and 750°C respectively for 2h. The samples *A*−Nb_2O_5, *B*−Nb_2O_5, *C*−Nb_2O_5 and *D*−Nb_2O_5 were prepared using the Pechini method adapted from previous procedures reported[18].

Niobium chloride ($NbCl_5$ 99% Sigma-Aldrich) was employed as the starting precursor, hydrated citric acid (99.5% Panreac) as a chelating agent and ethylene glycol (99.8% Panreac) as polymerizing agent. The employed solvents were: distilled water for the samples *A*−Nb_2O_5 and aqueous solutions of 65% HNO_3, 37% HCl and 30% NH_4OH for the samples *B*−Nb_2O_5, *C*−Nb_2O_5 and *D*−Nb_2O_5 respectively. The precalcination was performed at 300°C for 4 hours. The powders that were obtained were calcined at 500, 650 and 750°C for 2h respectively (table 2).

Sol-gel and Pechini methods were chosen for their similarity and since these allow the preparation of homogeneous and highly pure powders and porous and high surface area oxides, with fine particles and adequate chemical composition. The Pechini route consists of the formation of chelates between metal ions and carboxylic acids. These are subsequently polymerized by a reaction with polyalcohols, which have a good distribution of metallic ions in the polymer structure, that when heated at moderate temperatures it favors the condensation reaction causing polyesterification to occur. The excess water is removed and a homogeneous gel is formed[19,20]. The sol-gel method enables homogenous samples to be obtained at low temperatures and the starting cationic composition to be maintained by the use of metal salts as raw materials and mixing them in a liquid solution. The principal advantage of the Sol-gel method is that reagents are mostly mixed in atomic levels, which may increase the reaction rate and decrease the heat treatment temperature[21].

Table 1: Different conditions of the preparation samples in the sol-gel method.

sample	Hydrolysis	Temperature °C
1-Nb_2O_5 – 500°C	NH_4OH	500
2-Nb_2O_5 – 500°C	H_2O	
1-Nb_2O_5 – 650°C	NH_4OH	650
2-Nb_2O_5 – 650°C	H_2O	
1-Nb_2O_5 – 750°C	NH_4OH	750
2-Nb_2O_5 – 750°C	H_2O	

Table 2: Different conditions of the preparation samples in the Pechini method.

sample	Solvent	Temperature °C
A-Nb_2O_5 – 500°C	H_2O	500
B-Nb_2O_5 – 500°C	$H_2O - HNO_3$	
C-Nb_2O_5 – 500°C	$H_2O - HCl$	
D-Nb_2O_5 – 500°C	$H_2O - NH_4OH$	
A-Nb_2O_5 – 650°C	H_2O	650
B-Nb_2O_5 – 650°C	$H_2O - HNO_3$	
C-Nb_2O_5 – 650°C	$H_2O - HCl$	
D-Nb_2O_5 – 650°C	$H_2O - NH_4OH$	
A-Nb_2O_5 – 750°C	H_2O	750
B-Nb_2O_5 – 750°C	$H_2O - HNO_3$	
C-Nb_2O_5 – 750°C	$H_2O - HCl$	
D-Nb_2O_5 – 750°C	$H_2O - NH_4OH$	

The XRD patterns were obtained using two different methods. In the first term an Xpert-PRO PANalytical diffractometer (Co $K\alpha_1$ radiation, λ= 1.78901Å), operating at 40*mA*. A step of 0.0133° in 1 min, in the 2θ angle range of 10 – 90° was used. That equipment then required technical support. For the remaining analysis an Xpert PANalytical Empyrean Serie II Alpha 1 (Cu $K\alpha_2$) radiation, λ=1.54442Å) was used operating at 40*mA* with a step of 0.05° in 50 seconds, in the 2θ angle range of 5 – 80°. The identification of the

crystalline phases was performed using the X'Pert HighScore PANalytical software. Raman spectroscopy was made using a commercial micro-Raman probe setup TG4000 Jobin Yvon spectrometer (Raman excitation line: λ=532 nm) at room temperature. The Brunauer-Emmett-Teller (*BET*) approach was employed to determine the specific surface area of the nanosize powders, employing a Micromeritics ASAP 2020 − 77 K apparatus with adsorption data at a relative pressure range of 0.03 − 0.15. Before the analysis, each sample was outgassed at 100°C for 2 hours then the temperature was increased to until 300°C. The UV-vis spectra were taken using Cary 5000 spectrometer (varian) in diffuse reflection mode. A field emission scanning electron microscope (SEM Vega3 Tescan) operating at 5.0kV was used to verify the material morphology.

3. Results and discussion

Figure 1 *XRD* patterns peak analysis verifies that those Nb_2O_5 samples obtained by the Pechini method heated at 750°C have the orthorhombic crystalline structure due to the existence of dominant diffraction peaks according to PDF cards No. 30-0873 (contained in the Power Diffraction File) for the T-Nb_2O_5 phase, (a = 6, 175Å, b = 29, 175Å, c = 3, 930Å). The *XRD* patterns of the samples obtained by routes based on the Pechini method at 650°C also displayed the existence of the T-Nb_2O_5 phase although with less crystallinity. At 500°C spectra obtained from routes based on the Pechini method coincided with PDF cards No. 28-0317 for the low temperature pseudohexagonal TT-Nb_2O_5 phase (a = b = 3,607Å, c = 3.925Å).

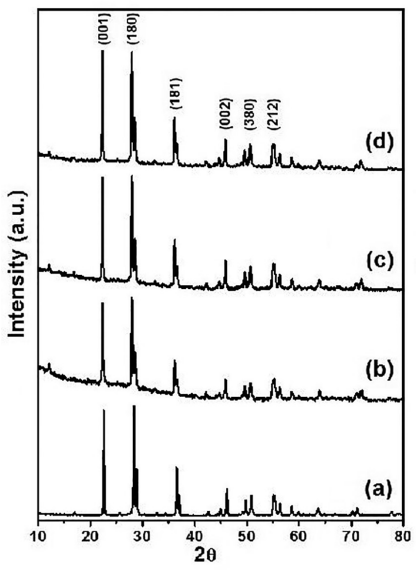

Figure 1: XRD diffraction patterns of samples obtained by Pechini method; the samples correspond to $T-Nb_2O_5$ phase obtained by heating at 750°C. (a) A-Nb_2O_5 – 750°C, (b)B-Nb_2O_5 – 750°C, (c) C-Nb_2O_5 – 750°C and (d) D-Nb_2O_5 – 750°C.

In Figure 2 *XRD* patterns of the Nb_2O_5 samples obtained by the Sol-gel method are presented. The sharpness and intensity of all diffraction peaks improve progressively with the increase in the calcination temperature which proves the crystallite growth of Nb_2O_5 nanoparticles. Figure 2 *XRD* patterns show that at 650 and 750°C the crystalline structures are orthorhombic according to PDF cards No. 30-0873. In the *XRD* patterns of the 1-Nb_2O_5 – 500°*C* and 2-Nb_2O_5 – 500°*C* samples there are no appreciable peaks that specify the crystalline phase that was reached. In general the *XRD* patterns structurally point out the pureness of the Nb_2O_5 nanosize powders synthesized by Pechini and Sol-gel methods due to the absence of undesired impurities generated from the precursors used in both methods.

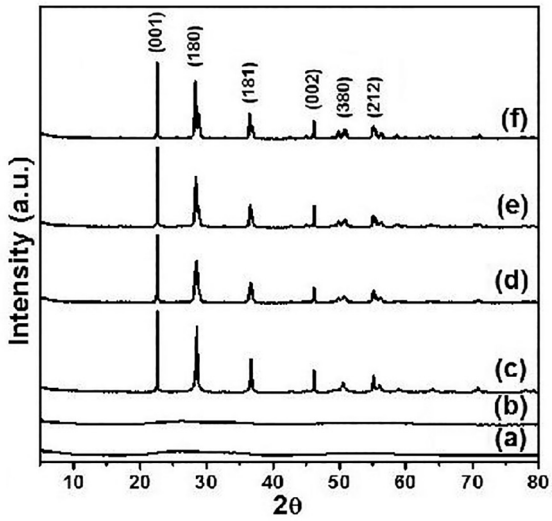

Figure 2: Sol-gel method, samples obtained by heating at 500, 650 and 750°C. (a) 1-Nb_2O_5 −500°C, (b) 2-Nb_2O_5 −500°C, (c) 1-Nb_2O_5 – 650°C, (d) 2-Nb_2O_5 −650°C, (e) 1-Nb_2O_5 −750°C and (f) 2-Nb_2O_5 – 750°C.

To analyze the crystallite growth, the crystallite size (L) of the Nb_2O_5 nanoparticles was calculated by the Scherrer's equation L = $K\lambda/(\beta cos\theta)$, (for peak broadening due to size effects) where K is the shape correction factor, 0.9 for L taken as the volume-averaged crystallite dimension perpendicular to the *hkl* diffraction plane; λ is the wavelength used, θ is the Bragg diffraction angle measured hkl peak and β represents the *FWHM* (Full width at half maximum) measured in radians on the 2θ scale[22]. The broadening lines chosen for the L estimate correspond to (001), (180), (181), (002), (380), and (212) crystalline planes according to PDF No. 01-071-0336 reported in Inorganic Crystal Structure Database (ICSD)[23]. The crystallite size of nanoparticles on the T-Nb_2O_5 phase increases from ~25 to ~65nm with an increase in calcination temperature, as shown table 3.

The crystallite size increases more with the A-Nb_2O_5 route than the C-Nb_2O_5 route; with the B-Nb_2O_5 and D-Nb_2O_5

Table 3: Crystallite size estimated by Scherrer equation from the XRD data

2θ	(hkl)	Crystallite size (nm)		
22.5	(001)	A-Nb_2O_5 – 500°C 11.1	A-Nb_2O_5 – 650°C 26.6	A-Nb_2O_5 – 750°C 66.4
36.6	(181)	12.7	30.6	50.9
22.5	(001)	C-Nb_2O_5 – 500°C 20.9	C-Nb_2O_5 – 65°C 29.1	C-Nb_2O_5 – 750°C 35.3
28.5	(180)	11.0	43.9	33.5
22.6	(001)		1-Nb_2O_5 – 65°C 54.5	1-Nb_2O_5 – 750°C 54.5
50.7	(380)		52.8	63.8
28.4	(180)		2-Nb_2O_5 – 65°C 25.4	2-Nb_2O_5 – 750°C 46.5
50.8	(380)		22.7	35.4

routes the crystallinity achieved at 650°C is very similar to that achieved at 750°C. The achieved crystallinity with 1-Nb_2O_5 route is more or less uniform at 650°C and 750°C while the crystallinity increases with the 2-Nb_2O_5 route when the samples are sintered at 650°C and 750°C. This is due to the fact that the crystallite size is greater when the hydrolisis is catalyzed in basic medium. The samples A-Nb_2O_5 – 750°C and 1- Nb_2O_5–750°C have the L larger. In general the route A of the Pechini method allows to obtain a larger crystallite size and 750°C is the more favorable crystallization temperature. Table 4 shows the results of specific surface area, S_{BET} determined by taking data at relative pressures between 0.03 and 0.15. The method had accuracy constraints during the measurement process. This fact was observed because the values of S_{BET} were less than $10m^2$/g. The S_{BET} dates show that the increase in the calcination temperature from 500°C to 750°C resulted in the progressive decrease of specific surface area of the Nb_2O_5 nanosize powders. This is mainly because a more high calcination temperature can lead to a greater proportion of the pore coalescence due to the further crystallization of walls separating mesopores in their structure which be established through measurement of pore size. The B route Pechini method did not show regularity in S_{BET} downward trend with increasing temperature, unlike *C* and *D* routes which did. S_{BET} of the samples obtained by Sol-gel method did not display a decrease with the temperature. The similarity between specific surface area of the C-Nb_2O_5 – 750°C, D-Nb_2O_5– 750°C and 2-Nb_2O_5– 750°C samples agree with the crystallinity achieved at 750°C and information compared with the *SEM* images show as small S_{BET} measurements are associated with larger particle sizes.

This fact is well consistent with the observed results of a higher crystallinity and a larger crystallite size of the Nb_2O_5 nanoparticles at a higher calcination temperature (figure 2 and figure 3). When comparing the data re- ported in table 4 with the *SEM* images it is concluded that the oxides prepared at 500°C by the method Pechini had a high S_{BET} because at this temperature the particle size is small.

Figure 3 shows SEM photographs of the selected samples sol-gel and Pechini. Figure 3 also shows the SEM micrographs of samples Nb_2O_5 by the Pechini (B and D) and sol-gel (1 and 2) method, at a temperature of 750°*C* respectively. The samples obtained by Sol-gel (1,2-Nb_2O_5) show a structure of the particles consisting of regular spherical particles of well-defined shapes and sizes of approximately 1-2 μm, figure 3 (a),(b). In figure 3(c) and (d) for example, two samples are presented for Pechini method. These samples exhibit the nanoparticles formation, whereas the SEM photograph of sample (a) and (b) shows a unique spherical microstructure. The last two photographs show high-magnification SEM images. Here, it is also shown that particles involved are smaller. This indicates that by virtue of Pechini method, smaller and irregular particles are obtained.

In Figure 4 (a), (c) UV-Vis $A-Nb_2O_5$ material is observed at different calcination temperatures. By extrapolating the linear part of a curve photon energy to the abscissa, the band gap energy transition can be derived. The band gap energies of the Pechini method, $A-Nb_2O_5$ were estimated to be 3.40, 3.32 and 3.32eV, respectively to different temperatures. This difference might be due to the different crystal sizes of the samples. The value of the band gap is also an indication that the calcination temperature influences the process for higher calcination temperatures, however the energy band is the same.

Table 4: S_{BET} values of the synthesized samples: sol-gel method 1 − 2 and Pechini *C* − *D*. The S_{BET} was determined by taking data at relative pressures between 0.03 and 0.15.

Sample	S_{BET} (m^2/g)	Sample	S_{BET} (m^2/g)	Sample	S_{BET} (m^2/g)
C-Nb_2O_5 – 500°C	79.50	C-Nb_2O_5 – 650°C	14.52	C-Nb_2O_5 – 750°C	4.53
D-Nb_2O_5 – 500°C	75.85	D-Nb_2O_5 – 650°C	9.85	D-Nb_2O_5 – 750°C	4.44
1-Nb_2O_5 – 500°C	1.70	1-Nb_2O_5 – 650°C	1.17	1-Nb_2O_5 – 750°C	1.19
2-Nb_2O_5 – 500°C	1.30	2-Nb_2O_5 – 650°C	14.24	2-Nb_2O_5 – 750°C	4.68

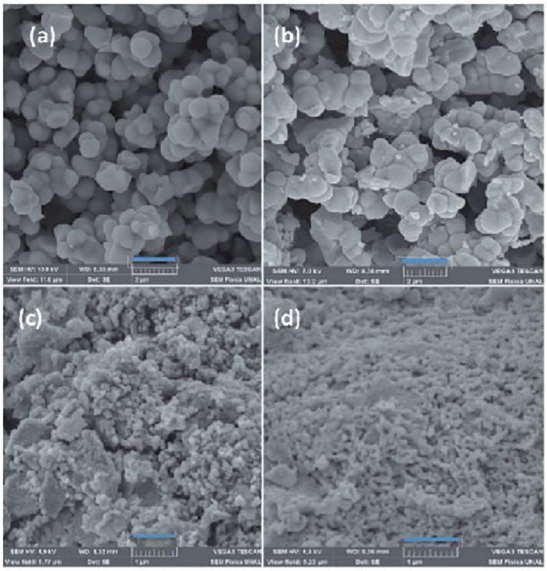

Figure 3: SEM micrographs of Nb_2O_5 particles: (a) 1-Nb_2O_5 −750°C for a resolution of 2µm, (b) 2-Nb_2O_5 – 750°C for a resolution of 2µm, 750°C for a resolution of 1µm.

Figure 5 (a)-(e) UV-Vis for samples to 750°*C* by sol- gel methods and Pechini. In literature, as a typical n-type wide band gap semiconductor (Eg═3.4eV), Nb_2O_5 is the most thermodynamically stable phase among various niobium oxides[24]. As shown in figure 5 the band gap energy values for different samples are very close to the value of literature between 3.32 and 3.37eV. Small changes in values can be related to particle size[25]. There is no clear explanation for the discrepancy of the band gap in this study. As can be seen, the energy band by the two methods of growth varies, being lower for the B method Pechini while it remained practically the same for the other methods. Rigorously, we believe the particle size and band gap depend on: method of preparation, calcination temperature and grain size.

Figure 6 shows the Raman spectra for samples C-Nb_20_5 by Pechini method at different calcination temperatures. As shown in figure 6 (a) and (b) the position of the Raman peaks is narrow and well defined which indicates crystallinity in the material of these calcination temperatures. In figure 6 (c) Raman modes for the calcination temperature of 500°*C* can be observed. This spectrum does not have well-defined peaks which indicates an amorphous or poorly crystalline material. Bands corresponding to vibrations of cations occupying centres of octahedrons and tetrahedrons are found in the 150-400cm^{-1} range[26-28]. In the spectrum of Figure 6 (a-b), the peaks occur at 78.3, 127.4, 227.3 and 307.4cm^{-1}. Bands of the oxygen framework vibrations are located in the 500-1100cm^{-1} range, figure 6(a-b) at 521, 642.6, 689.3 and 843cm^{-1}. With the decrease of the calcination temperature, the peaks decrease rapidly.

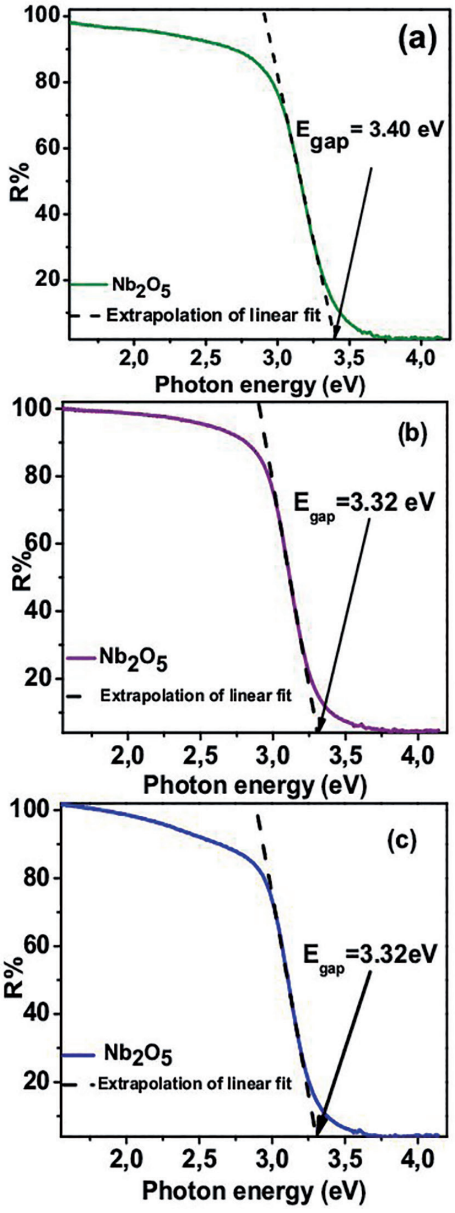

Figure 4: UV-Vis Spectra of Nb_2O_5 nanoparticles synthesized by the Pechini method (A-Nb_2O_5) at different temperatures: (a) 500, (b) 650 and (c) 750°C.

Figure 7 (a) and (b) shows the Raman spectra of sample 2-Nb_2O_5 by Sol-gel method. For Irena *et al.*[29] the bands in the 400 - 800cm^{-1} wavenumber region are assigned to the symmetric and antisymmetric stretching mode of the Nb-O-Nb linkage. While the Raman band at 235cm^{-1} becomes the bending mode of Nb-O-Nb. The spectra in figure 7, corresponds to a well developed crystalline structure of Nb_2O_5. As shown in figure 6 compared to figure 7 the Raman modes are narrower, also the peak near 667cm^{-1} is much more intense. These two figures again show that the calcination temperature of 700°*C* is ideal for crystalline samples. In general the Raman study

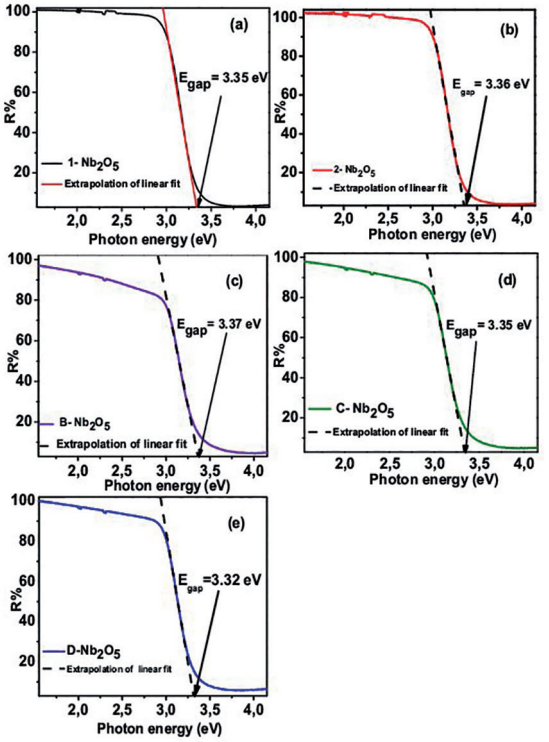

Figure 5: UV-Vis Spectra of Nb_2O_5 nanoparticles at temperature of 750°C. (a) 1-Nb_2O_5 – 750°C, (b) 2-Nb_2O_5 – 750°C, (c) B-Nb_2O_5 – 75°C, (d) C-Nb_2O_5 – 750°C and (e) D-Nb_2O_5 – 750°C.

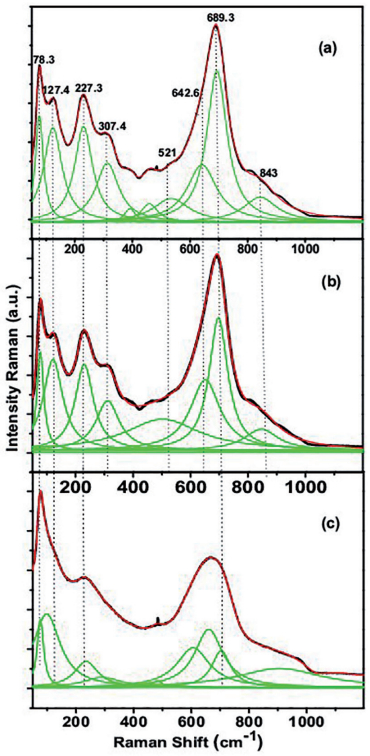

Figure 6: Raman spectra for C-Nb_2O_5 at (a) 750°C, (b) 650°C and (c) 500°C.

shows that an increase of the synthesis temperature causes an increase in the material crystallinity because an increase in the synthesis temperature led to a sharp peak, this fact is verified with the values of the crystallite size that were estimated by the Scherrer equation (Table 3).

4. Conclusions

The microstructure of the resulting $T-Nb_2O_5$ nanosize powder is linked to the two synthesis methods, because the properties of the niobium oxide powders are strongly dependent on the raw material and on the synthesis route used. The employed Pechini and Sol- gel routes allowed the preparation of Nb_2O_5 nanosize powders. For heat treatment temperatures about 500°C the powder has a $TT-Nb_2O_5$ phase. The heat treatment process allows the formation of $T-Nb_2O_5$ nanosize powders with an orthorhombic structure, which was confirmed by *XRD*. The Raman spectroscopy technique confirmed the phase transformations observed by X-ray diffraction. In the *SEM* it was observed that the grain size is smaller for the Pechini method, but for the sol gel method it is more uniformed. As is been in the UV-VIS measurements confirmed that with the increase of the calcination temperature decreases the $E_{gap.}$

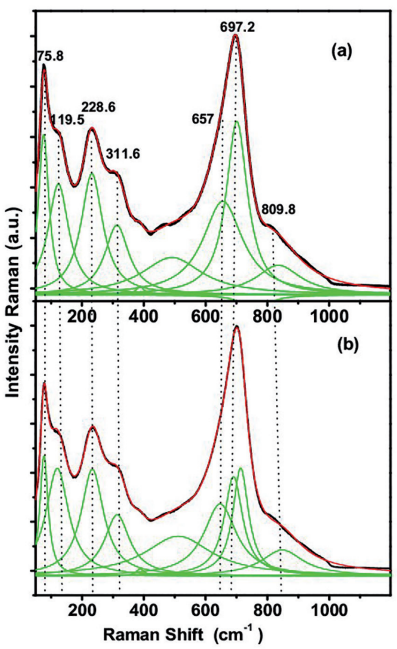

Figure 7: Raman spectra for 2-Nb_2O_5 sol-gel method (a) 750º C and (b) 650º C.

5. Acknowledgements

Authors acknowledge financial support from the agencies; Universidad Francisco de Paula Santander, Cúcuta, Colombia; Universidad Nacional Colombia and Colciencias and CNPq Brazil.

6. References

1. Wang YD, Yang LF, Zhou ZL, Li YF, Wu XH. Effects of calcining temperature on lattice constants and gas-sensing properties of Nb_2O_5. *Materials Letters*. 2001;49(5):277-281.

2. Mujawar SH, Inamdar AI, Patil SB, Patil PS. Electrochromic properties of spray-deposited niobium oxide thin films. *Solid State Ionics*. 2006;177(37-38):3333-3338.

3. Jose R, Thavasi V, Ramakhrisna S. Metal Oxides for Dye-Sensitized Solar Cells. *Journal of the American Ceramic Society*. 2009;92(2):289-301.

4. Lira-Cantu M, Krebs FC. Hybrid solar cells based on MEH-PPV and thin film semiconductor oxides (TiO_2, Nb_2O_5, ZnO, CeO_2 and CeO_2–$CTiO_2$): Performance improvement during long-time irradiation. *Solar Energy Materials and Solar Cells*. 2006;90(14):2076-2086.

5. Ahn KS, Kang MS, Lee JK, Shin BC, Lee JW. Enhanced electron diffusion length of mesoporous TiO_2 film by using Nb_2O_5 energy barrier for dye-sensitized solar cells. *Applied Physics Letters*. 2006;89:013103.

6. Hashemzadeh F, Gaffarimejad A, Rahimi R. Porous *p*-NiO/*n*-Nb_2O_5 nanocomposites prepared by an EISA route with enhanced photocatalytic activity in simultaneous Cr(VI) reduction and methyl orange decoloration under visible light irradiation. *Journal of Hazardous Materials*. 2015;286:64-74.

7. Carniti P, Gervasini A, Marzo M. Dispersed NbO*x* Catalytic Phases in Silica Matrixes: Influence of Niobium Concentration and Preparative Route. *The Journal of Physical Chemistry C*. 2008;112(36):14064-14074.

8. Sreethawong T, Ngamsinlapasathian S, Lim SH, Yoshikawa S. Investigation of thermal treatment effect on physicochemical and photocatalytic H_2 production properties of mesoporous-assembled Nb_2O_5 nanoparticles synthesized via a surfactant-modified sol–gel method. *Chemical Engineering Journal*. 2013;215-216:322-330.

9. Marin ML, Hallett-Tapley GL, Impellizzeri S, Fasciani C, Simoncelli S, Netto-Ferreira JC, et al. Synthesis, acid properties and catalysis by niobium oxide nanostructured materials. *Catalysis Science & Technology*. 2014;4:3044-3052.

10. Zhao Y, Zhou X, Ye L, Tsang SCE. Nanostructured Nb_2O_5 catalysts. *Nano Reviews*. 2012;3:17631.

11. Soares MRN, Leite S, Nico C, Peres M, Fernandes AJS, Graça MPF, et al. Effect of processing method on physical properties of Nb_2O_5. *Journal of the European Ceramic Society*. 2011;31(4):501-506.

12. Rani RA, Zoolfakar AS, O'Mullane AP, Austin MW, Kalantar-Zadeh K. Thin films and nanostructures of niobium pentoxide: fundamental properties, synthesis methods and applications. *Journal of Materials Chemistry A*. 2014;2(38):15683-15703.

13. Rosario AV, Pereira EC. Influence of the crystallinity on the Li^+ intercalation process in Nb_2O_5 films. *Journal of Solid State Electrochemistry*. 2005;9(10):665-673.

14. Lopes OF, Paris EC, Ribeiro C. Synthesis of Nb_2O_5 nanoparticles through the oxidant peroxide method applied to organic pollutant photodegradation: A mechanistic study. *Applied Catalysis B: Environmental*. 2014;144:800-808.

15. Graça MPF, Meireles A, Nico C, Valente MA. Nb_2O_5 nanosize powders prepared by sol–gel Structure, morphology and dielectric properties. *Journal of Alloys and Compounds*. 2013;553:177-182.

16. Ristić M, Popović S, Musić S. Sol–gel synthesis and characterization of Nb_2O_5 powders. *Materials Letters*. 2004;58(21):2658-2663.

17. Uekawa N, Kudo T, Mori F, Wu YJ, Kakegawa K. Low-temperature synthesis of niobium oxide nanoparticles from peroxo niobic acid sol. *Journal of Colloid and Interface Science*. 2003;264(2):378-384.

18. Raba AM, Barba-Ortega J, Joya MR. The effect of the preparation method of Nb_2O_5 oxide influences the performance of the photocatalytic activity. *Applied Physics A*. 2015;119(3):923-928.

19. Bouquet V, Longo E, Leite ER, Varela JA. Influence of heat treatment on $LiNbO_3$ thin films prepared on Si(111) by the polymeric precursor method. *Journal of Materials Research*. 1999;14(7):3115-3121.

20. Pechini MP, inventor; Sprague Electric Co, assignee. Method of preparing lead and alkaline earth titanates and niobates and coating method using the same to form a capacitor. United States patent US 3330697 A. 1967 Jul 11.

21. Galceran M, Pujol MC, Aguillo´ M, Díaz F. Sol- gel modified Pechini method for obtaining nanocrystalline $KRE(WO_4)_2$ (RE = Gd and Yb). *Journal of Sol-Gel Science and Technology*. 2007;42(1):79-88.

22. Kato K, Tamura S. Die Kristallstruktur von T-Nb_2O_5. *Acta Crystallographica Section B*. 1975;B31:673-677.

23. Ikeya T, Senna M. Change in the structure of niobium pentoxide due to mechanical and thermal treatments. *Journal of Non-Crystalline Solids*. 1988;105(3):243-250.

24. Liu J, Xue D, Li K. Single-crystalline nanoporous Nb_2O_5 nanotubes. *Nanoscale Research Letters*. 2011;6:138.

25. Cavalcante LS, Marques VS, Sczancoski JC, Escote MT, Joya MR, Varela JA, et al. Synthesis, structural refinement and optical behavior of $CaTiO_3$ powders: A comparative study of processing in different furnaces. *Chemical Engineering Journal*. 2008;143(1-3):299-307.

26. Jehng JM, Wachs IE. Structural chemistry and Raman spectra of niobium oxides. *Chemistry of Materials*. 1991;3(1):100-107.

27. Bormanis K, Palatnikov M, Shcherbina O, Frolov A, Chufyrev P, Sidorov N. Physical Properties and Structure of Niobium Pentoxide Ceramics Treated by Concentrated Light Flow. *Integrated Ferroelectrics*. 2011;123(1):137-143.

28. Brayner R, Bozon-Verduraz F. Niobium pentoxide prepared by soft chemical routes: morphology, structure, defects and quantum size effect. *Physical Chemistry Chemical Physics*. 2003;5:1457-1466.

29. Mickova I. Photoelectrochemical Study of Anodically Formed Oxide Films on Niobium Surfaces. *Croatica Chemica Acta*. 2010;83(2):113-120.